Robust Joint Multi-Antenna Spoofing Detection and Attitude Estimation using Direction Assisted Multiple Hypotheses RAIM

Michael Meurer, Andriy Konovaltsev, Manuel Cuntz, Christian Hättich,
Institute of Communications and Navigation, German Aerospace Center (DLR)
Oberpfaffenhofen, Germany

BIOGRAPHY

Michael Meurer received the diploma in electrical engineering and the Ph.D. degree from the University of Kaiserslautern, Germany. After graduation, he joined the Research Group for Radio Communications at the Technical University of Kaiserslautern, Germany, as a senior key researcher, where he was involved in various international and national projects in the field of communications and navigation both as project coordinator and as technical contributor. From 2003 till 2005, Dr. Meurer was active as a senior lecturer. Since 2005 he has been an Associate Professor (PD) at the same university. Additionally, since 2006 Dr. Meurer is with the German Aerospace Centre (DLR), Institute of Communications and Navigation, where he is the director of the Department of Navigation and of the center of excellence for satellite navigation.

Andriy Konovaltsev received his engineer diploma and the Ph.D. degree in electrical engineering from Kharkov State Technical University of Radio Electronics, Ukraine in 1993 and 1996, correspondingly. He joined the Institute of Communications and Navigation of DLR in 2001. His main research interest is in application of antenna array signal processing for improving performance of satellite navigation systems in challenging signal environments.

Manuel Cuntz received the diploma in electrical engineering degree in 2005 from the Technical University of Kaiserslautern. He joined the Institute of Communications and Navigation of DLR in June 2006. His fields of research are multi-antenna satellite navigation receivers.

Christian Hättich received his Master of Science in Embedded Systems in 2011 from HS Pforzheim University. Since March 2011, he is working at the Institute of Communications and Navigation of DLR. His current research interests are multi-antenna receivers and robust navigation signal processing.

ABSTRACT

The paper presents an approach for detection of spoofing/meaconing signals using the direction-of-arrival (DOA) measurements available in a multi-antenna navigation receiver. The detection is based on comparison and statistically testing of the measured DOAs against the expected DOAs. The expected DOAs are computed in the receiver using the almanac and ephemeris information while performing the estimation of the user position. The attitude of the antenna array is assumed to be unknown and therefore has to be estimated as well. Consequently, the detection of spoofing/meaconing signals using this approach is treated as a joint detection/estimation problem. The solution to this problem is described in this paper. In addition, the performance of the proposed approach is analyzed through simulations in exemplary artificial scenarios and by processing real DOA measurement data collected during measurement campaigns.

INTRODUCTION

Radio frequency interference is one of the major concerns for safety-critical applications of global satellite navigation systems (GNSSs). This phenomenon can be classified into two types of interference: (i) jamming that aims to prevent a receiver from using the satellite signals for navigation and (ii) spoofing or meaconing aiming to fool a receiver, which can result in a wrong position and/or time solution. The spoofing and meaconing signals can arise intentionally or unintentionally. For example, improperly used GPS repeaters/re-radiators which are originally meant for improving indoor availability of GNSS can act as a source of meaconing [1].

Until recently, spoofing and meaconing of GNSS signals have only been considered relevant and of interest in the frame of military applications. However, it turns out that this threat also gains more and more attention in other fields especially in the context of safety and security critical applications. Therefore the reliable detection and mitigation of this threat is of major interest for a large variety of applications.

Multi-antenna processing in a GNSS receiver is a valuable technique for identifying spoofing, meaconing as well as multipath signals. The use of such a technique allows for identification of the directions of arrival (DOAs) of incoming signals with the help of high-resolution direction finding methods like MUSIC and ESPRIT which have accuracies in the order of a few degrees or better [2], [3], [4]. As the expected DOAs of GNSS signals can be obtained from GNSS almanac data [5] or other side information channels, comparing the estimated directions of arrival with the expected ones allows identifying spoofing/meaconing signals or multipath echoes, which typically arrive from directions of arrival different from those of the direct GNSS satellite signals. Since the DOA estimation delivers results in the local coordinate frame of the antenna array, the estimated DOAs have to be transformed into a GNSS local geodetic coordinate frame before being used for the spoofing/meaconing identification. This conversion requires sufficiently accurate knowledge of the attitude of the receiving antenna array platform. Especially for mobile GNSS receivers on vehicles, ships and aircraft the autonomous (e.g. without the use of external sensors) determination of the attitude of the multi-antenna platform is a challenging task, since it needs to be updated continuously and instantly even under high dynamics of the mobile platform and the presence of spoofing/meaconing signals.

This paper solves the aforementioned problem by treating the process of spoofing detection and attitude estimation as a joint detection/estimation problem. For this reason, it is assumed that several GNSS signals are received by a multi-antenna receiver where each signal is associated with an individual combination of the satellite navigation system (e.g. GPS / Galileo etc.) and PRN code. Furthermore, at least one direction of arrival is observed for each such combination. In case of spoofing, meaconing or multipath propagation multiple directions of arrival may correspond to a single GNSS signal. In the undisturbed case, the attitude determination for the antenna array platform could be completed in three following steps: In the first step, all directions of arrival of the incoming GNSS signals are estimated in the local coordinate frame of the antenna array platform with the help of the DOA estimation technique. In the second step, the expected DOAs of all GNSS signals are determined in the local East, North, Up (ENU) Cartesian coordinates by using side information like the system almanac. And finally in the third step, the attitude of the multi-antenna array platform is determined on the basis of the estimated DOAs in the local coordinate frame and the expected DOAs in the ENU frame. The challenge during this process is the fact that spoofing /meaconing signals may hamper the correct determination of the attitude and lead to wrong attitude estimation results. Moreover, if more than one, i.e. N, different directions of arrival per signal are available, obviously $N-1$ or even all N directions are not associated with the real line-of-sight propagation

path between the GNSS satellite and the GNSS receiver and, therefore, are useless for attitude determination. Thus, a straight sequential process of attitude estimation as a first step and the spoofing determination following afterwards is not possible.

Within the joint spoofing detection and attitude estimation process these restrictions are taken into account. An approach with similarities to multiple hypotheses RAIM [6] is used where a multitude of hypotheses is followed in parallel. Each hypothesis contains an assumption about which GNSS signals and corresponding DOAs are trustworthy and which are not trustworthy due to spoofing, meaconing or simple multipath propagation. For each hypothesis an estimate of the attitude of the GNSS antenna platform as well as an associated test metric indicating likelihood of this hypothesis are determined. Based on the test results for several hypotheses the following can be determined: (i) the most likely estimate of the attitude of the multi-antenna array platform and (ii) the most likely decision about which GNSS signals and DOAs are correct and which are incorrect due to spoofing, meaconing and multipath. The process of establishing, tracking and discarding hypotheses as well as the estimation of the attitude of the antenna array is an iterative procedure.

The paper is organized as follows. The next section of the paper is dedicated to the derivation and description of the novel joint spoofing detection and attitude estimation process. Further in the third section, the potential performance of the proposed approach is analyzed by simulations using exemplary artificial scenarios. In order to assess the performance of the approach in practical scenarios, real DOA measurements which have been collected during measurement campaigns using the multi-antenna GNSS receiver developed by the German Aerospace Center (DLR) [2] will also be used. Finally, the paper will be concluded by summarizing the results of this study drawing several conclusions.

THEORETICAL DERIVATIONS

The mathematic model for the observations of the directions of arrival of satellite signals, which are obtained by a DOA estimation technique of the antenna array signal processing can be written as follows

$$\mathbf{D}_{loc} = \mathbf{M}(r, p, y)\mathbf{D}_{enu} + \mathbf{N} \qquad (1)$$

where

$\mathbf{D}_{loc}$ is a $[3 \times N_{\text{DOA}}]$ matrix composed of N_{DOA} unit vectors of directional cosines corresponding to the directions of arrival of satellite signals in the local coordinate frame of the antenna array. A single directional cosine vector is defined as $\hat{\mathbf{d}}_{loc} = [\sin\theta\cos\varphi, \sin\theta\sin\varphi, \cos\theta]^{\text{T}}$, where θ is an elevation angle and φ is an

azimuth angle in the antenna local coordinate frame (see Figure 1);

$\mathbf{D}_{enu}$ is a $[3 \times N_{\text{DOA}}]$ matrix composed of unit vectors of directional cosines corresponding to the DOAs of satellite signals in the user local ENU coordinate frame (see Figure 2). The directional cosine vector is defined in this coordinate frame as follows

$$\widehat{\boldsymbol{d}}_{enu} = [\cos El \sin Az, \cos El \cos Az, \sin El]^{\text{T}}$$

where El and Az are the elevation and azimuth angles, correspondingly, in the ENU coordinate frame;

$\mathbf{M}(r, p, y)$ is a $[3 \times 3]$ unitary rotation matrix (see [7], p.441) corresponding to the attitude of the antenna array defined by three Eulers angles: roll r, pitch p and yaw y. These angles are referred to the user local ENU coordinate frame;

$\mathbf{N}$ is a $[3 \times N_{\text{DOA}}]$ matrix describing the measurement noise effect.
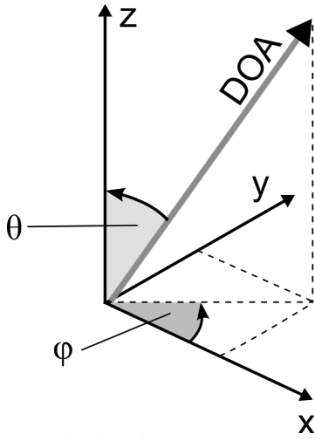

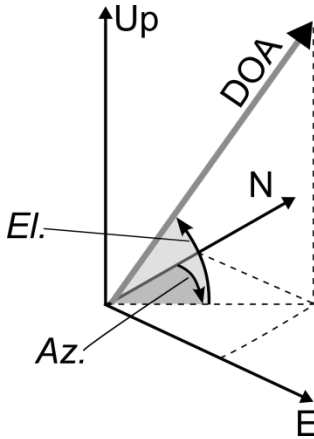Figure 1: DOA in local antenna coordinate frame

Figure 2: DOA in geodetic East, North, Up (ENU) local coordinate frame

The relationship between the antenna coordinate frame and the ENU geodetic local coordinate frame is shown in Figure 3.
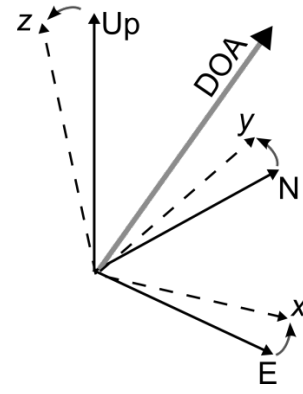

Figure 3: Local antenna and ENU coordinate frames

Examining the proposed mathematical model, one can see that the antenna array attitude can be estimated by solving the system of vector-matrix equations for three Euler angles in the least squares sense. This system of equations is typically overdetermined since at least 4 satellites are required to perform the PVT solution. The least squares problem is formulated as follows

$$(\hat{r}, \hat{p}, \hat{y}) = \underset{r,p,y}{\arg \min} \|\mathbf{M}(r, p, y)\mathbf{D}_{enu} - \mathbf{D}_{loc}\|^2 . \qquad (2)$$

The formulation of (2) is equivalent to the following minimization problem

$$(\hat{r}, \hat{p}, \hat{y}) =$$
$$= \underset{r,p,y}{\arg \min} \operatorname{trace}\{(\mathbf{M}(r, p, y)\mathbf{D}_{enu} - \mathbf{D}_{loc})^{\text{T}} \cdot$$
$$(\mathbf{M}(r, p, y)\mathbf{D}_{enu} - \mathbf{D}_{loc})\}. \qquad (3)$$

After performing matrix multiplications, the argument of trace function can be written in the following short form

$$\operatorname{trace}\{(\mathbf{M}(r, p, y)\mathbf{D}_{enu} - \mathbf{D}_{loc})^{\text{T}} \cdot$$
$$(\mathbf{M}(r, p, y)\mathbf{D}_{enu} - \mathbf{D}_{loc})\} =$$
$$= \operatorname{trace}\{\mathbf{D}_{enu}^{\text{T}} \mathbf{M}^{\text{T}}(r, p, y)\mathbf{M}(r, p, y)\mathbf{D}_{enu})\}$$
$$-\operatorname{trace}\{\mathbf{D}_{enu}^{\text{T}}\mathbf{M}^{\text{T}}(r, p, y)\mathbf{D}_{loc}\}$$
$$-\operatorname{trace}\{\mathbf{D}_{loc}^{\text{T}}\mathbf{M}(r, p, y)\mathbf{D}_{enu}\}$$
$$+\operatorname{trace}\{\mathbf{D}_{loc}^{\text{T}}\mathbf{D}_{loc}\}$$
$$= 2N_{\text{DOA}} - 2\operatorname{trace}\{\mathbf{D}_{enu}^{\text{T}}\mathbf{M}^{\text{T}}(r, p, y)\mathbf{D}_{loc}\} \qquad (4)$$

Taking this into account, the solution of the least squares problem of (2) leads to the maximization of the following cost function

$$(\hat{r}, \hat{p}, \hat{y}) = \underset{r,p,y}{\arg \max} \operatorname{trace}\{\mathbf{D}_{enu}^{\text{T}}\mathbf{M}^{\text{T}}(r, p, y)\mathbf{D}_{loc}\} \qquad (5)$$

or equivalently

$$(\hat{r}, \hat{p}, \hat{y}) = \underset{r,p,y}{\arg \max} \operatorname{trace}\left\{\mathbf{M}(r, p, y) \cdot \underbrace{\mathbf{D}_{enu}\mathbf{D}_{loc}^{\text{T}}}_{=\mathbf{C}}\right\} \qquad (6)$$

where $\mathbf{C} = \mathbf{D}_{enu}\mathbf{D}_{loc}^{\text{T}}$.

The maximum of the resulting cost function $J(r, p, y) = \text{trace}\{\mathbf{M}(r, p, y)\mathbf{C}\}$ of three Euler angles can be found by taking partial derivatives of the function and solving the following system of equations

$$\begin{cases} \text{trace}\left(\dfrac{\partial \mathbf{M}(r,p,y)}{\partial r}\mathbf{C}\right) = 0 \\[2mm] \text{trace}\left(\dfrac{\partial \mathbf{M}(r,p,y)}{\partial p}\mathbf{C}\right) = 0 \\[2mm] \text{trace}\left(\dfrac{\partial \mathbf{M}(r,p,y)}{\partial y}\mathbf{C}\right) = 0 \end{cases} \tag{7}$$

or, in a compact form

$$\begin{cases} g_r(r, p, y) = 0 \\ g_p(r, p, y) = 0 \\ g_y(r, p, y) = 0 \end{cases} \tag{8}$$

and

$$\mathbf{g}(r, p, y) = \begin{pmatrix} g_r(r, p, y) \\ g_p(r, p, y) \\ g_y(r, p, y) \end{pmatrix} = 0. \tag{9}$$

The components of the vector $\mathbf{g}(r, p, y)$ in (9) are non-linear functions of the Euler angles. In order to be able to iterative solve the given system of non-linear equations, the vector function $\mathbf{g}(r, p, y)$ can be linearized around the neighborhood of some starting point (r_0, p_0, y_0) using the Taylor expansion to the first order:

$$\mathbf{g}(r, p, y) \cong$$
$$\mathbf{g}(r_0, p_0, y_0) + [\nabla \mathbf{g}^{\mathrm{T}}(r_0, p_0, y_0)\,]^{\mathrm{T}}\begin{pmatrix} r - r_0 \\ p - p_0 \\ y - y_0 \end{pmatrix} \tag{10}$$

where ∇ is a vector differential operator defined as

$$\nabla = \left(\frac{\partial}{\partial r} \quad \frac{\partial}{\partial p} \quad \frac{\partial}{\partial y}\right)^{\mathrm{T}} \tag{11}$$

so that the gradient term $[\nabla \mathbf{g}^{\mathrm{T}}(r_0, p_0, y_0)\,]^{\mathrm{T}}$ produces the following $[3 \times 3]$ matrix

$$[\nabla \mathbf{g}^{\mathrm{T}}(r_0, p_0, y_0)\,]^{\mathrm{T}} =$$
$$= \begin{bmatrix} \dfrac{\partial g_r(r,p,y)}{\partial r} & \dfrac{\partial g_r(r,p,y)}{\partial p} & \dfrac{\partial g_r(r,p,y)}{\partial y} \\[3mm] \dfrac{\partial g_p(r,p,y)}{\partial r} & \dfrac{\partial g_p(r,p,y)}{\partial p} & \dfrac{\partial g_p(r,p,y)}{\partial y} \\[3mm] \dfrac{\partial g_y(r,p,y)}{\partial r} & \dfrac{\partial g_y(r,p,y)}{\partial p} & \dfrac{\partial g_y(r,p,y)}{\partial y} \end{bmatrix}. \tag{12}$$

The iterative formulation for the solution of the problem at hand is then as follows

$$\begin{pmatrix} r_{n+1} \\ p_{n+1} \\ y_{n+1} \end{pmatrix} =$$
$$\begin{pmatrix} r_n \\ p_n \\ y_n \end{pmatrix} - ([\nabla \mathbf{g}^{\mathrm{T}}(r_0, p_0, y_0)\,]^{\mathrm{T}})^{-1}\mathbf{g}(r_n, p_n, y_n). \tag{13}$$

The starting point (r_0, p_0, y_0) for the iterative solution in (13) can be obtained by solving the following least squares problem for an estimation of the rotation matrix $\widehat{\mathbf{M}}(r, p, y)$:

$$\widehat{\mathbf{M}}(r, p, y) = \underset{\widehat{\mathbf{M}}}{\operatorname{argmin}}\left\|\widehat{\mathbf{M}}(r, p, y)\mathbf{D}_{enu} - \mathbf{D}_{loc}\right\|^2. \tag{14}$$

The formulation of (14) is obtained by neglecting the side condition $\mathbf{M}(r, p, y)\mathbf{M}^{\mathrm{T}}(r, p, y) = \mathbf{I}$ which originates from the definition of a rotation matrix. The first estimation of the Euler angles can be obtained by using the elements of the resulting matrix $\widehat{\mathbf{M}}(r, p, y)$ as follows [7]:

$$\tan r_0 = -\frac{\widehat{M}_{13}}{\widehat{M}_{33}}$$

$$\tan p_0 = -\frac{\widehat{M}_{23}}{\sqrt{\widehat{M}_{21}^2 + \widehat{M}_{22}^2}} \tag{15}$$

$$\tan y_0 = -\frac{\widehat{M}_{21}}{\widehat{M}_{22}}.$$

The Gauss-Markov least squares solution of (12) is given by

$$\widehat{\mathbf{M}}(r, p, y) = \mathbf{D}_{loc}\mathbf{R}_N^{-1}\mathbf{D}_{enu}^{\mathrm{T}}(\mathbf{D}_{enu}\mathbf{R}_N^{-1}\mathbf{D}_{enu}^{\mathrm{T}})^{-1}, \tag{16}$$

where $\mathbf{R}_N$ is the covariance matrix of (12) the measurement noise.

The least squares problem formulated by (12) for estimating the rotation matrix is known in the literature as Wahba's problem. A computationally effective solution to this problem, and therefore also for determining the starting point of (11), is available by using the singular value decomposition (SVD) technique as described in [8].

By using equations (13), (15) and (16) the antenna array attitude can be determined as described above for a given set of DOA antenna measurements $\mathbf{D}_{loc}$ and the corresponding set of DOAs $\mathbf{D}_{enu}$ calculated with the GNSS system almanac data. The quality of the obtained solution for the attitude can be assessed using the sum of squares of errors (SSE) test statistics similar to how it is used with receiver autonomous integrity monitoring (RAIM) techniques [9], [10]. The SSE metric is defined as follows

$$SSE = \text{trace}\{[\mathbf{M}(r,p,y)\mathbf{D}_{enu} - \mathbf{D}_{loc}]^{\text{T}} \cdot$$
$$\mathbf{R}_N^{-1} [\mathbf{M}(r,p,y)\mathbf{D}_{enu} - \mathbf{D}_{loc}]\}, \qquad (17)$$

where the inverse of the covariance matrix of the measurement noise $\mathbf{R}_N^{-1}$ is used for normalizing individual error components (i.e. the residuals of the least squares solution).

If the antenna measurements for GNSS signal directions of arrival and the corresponding predicted DOAs are consistent with each other, the residuals of the least squares solution are unbiased and have zero mean. In this case the SSE metric as defined by (17) follows a central chi-squared distribution with $k = (2N_{\text{DOA}} - 3)$ degrees of freedom. In another case, when some measured directions of arrival are not consistent with the expected ones, the residuals of the least squares solution become biased and the SSE metric follows a non-central chi-squared distribution with the same number of degrees of freedom as in the error-free case but with some non-zero non-centrality parameter λ:

$$H_0(\text{no error}): \ SSE \sim \chi^2(k)$$
$$H_1(\text{error}): \qquad SSE \sim \chi'^2(k, \lambda)$$
$$k = (2N_{\text{DOA}} - 3) \qquad\qquad (18)$$
$$\lambda = \sum_{n=1}^{N_{\text{DOA}}} \left(\frac{\Delta_n}{\sigma_n}\right)^2$$

where

Δ_n is a bias in the n-th DOA measurement performed by the antenna array, this bias is expressed in (18) as an angle ψ between two direction cosines vectors of the measured DOA $\widehat{\boldsymbol{d}}_{loc}$ and the expected "almanac" DOA $\widehat{\boldsymbol{d}}_{enu}$. This angle between can be calculated as

$$\psi = \arccos(\widehat{\boldsymbol{d}}_{loc}^{\text{T}} \widehat{\boldsymbol{d}}_{enu}). \qquad (19)$$

σ_n is the standard deviation of the n-th DOA measurement error referred to the angle ψ between the vectors $\widehat{\boldsymbol{d}}_{loc}$ and $\widehat{\boldsymbol{d}}_{enu}$.

Examples of probability density functions (pdfs) of the SSE test statistics for H_0 and H_1 cases are shown in Figure 4. These theoretical results are obtained assuming availability of DOA antenna array measurements for 7 GNSS satellites. The assumed standard deviation σ_n of the angular errors of DOA measurements is 3°.
As it can be observed in Figure 4, the pdfs for H_0 and H_1 hypotheses becomes clearly separated at values of the non-centrality parameter $\lambda = 49$ or larger. If a single inconsistent signal is observed under adopted assumptions (i.e. number of DOA measurements, std of measurement error etc.) this signal with an inconsistent direction of arrival can be effectively detected if the angular

separation between the actual DOA and the expected "almanac" DOA is larger than 21° ($\sigma_n = 3°$, $\Delta_{spoofer}/\sigma_n = 7$). The detection of the spoofer/meaconing signal can be, for example, performed by using the Neyman-Pearson criterion [11], i.e. by setting a detection threshold defined by some desired false alarm rate.
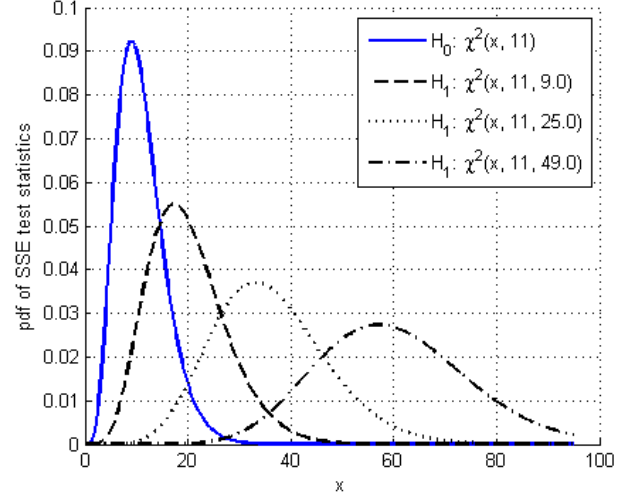

Figure 4: Probability distribution functions of SSE metric without outliers (H_0) and with outliers (H_1) in direction of arrival measurements for 7 satellites

The process of the joint attitude determination and spoofer (meaconing, multipath) detection/exclusion can be performed in following steps:

1. Test the hypothesis H_0:
   - Obtain an estimation of the antenna attitude together with the associated SSE test statistics.
   - Compare the test statistics against a predefined threshold. The threshold can be defined, for example, by a desired false alarm rate using the Neyman-Pearson criterion.
   - If the test statistics is below or equal to the threshold, the process is terminated. The determination of the antenna attitude is declared to be successful, no erroneous DOAs are detected.
   - If the SSE test statistics is larger than the threshold, the assumed number of erroneous DOA measurements is set to 1, i.e. $N_{err} = 1$, and the next steps are carried out.
2. Form N_{hyp} sub-sets (see) of DOA measurements corresponding to all possible H_1 hypotheses for the given number N_{err}, i.e. $N_{hyp} = \binom{N_{DOA}}{N_{err}}$.
3. Find the sub-set that delivers the minimum SSE test statistics:
   - Estimate the antenna attitude together with the associated SSE test statistics for each sub-set.
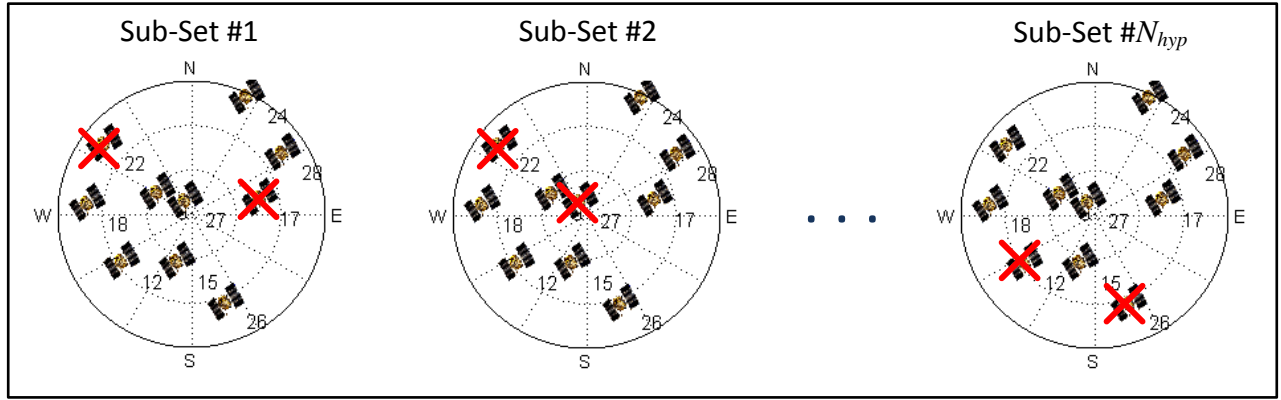
Figure 5: Example of sub-sets of DOA measurements for $N_{err} = 2$, $N_{\text{DOA}} = 10$ and $N_{hyp} = 45$

- Update the threshold by taking into account current value of N_{err}.
- If the obtained minimum test statistics is below or equal to the threshold, the process is terminated. The determination of the antenna attitude is declared to be successful. The GNSS signals which are excluded in the "winning" sub-set are reported as suspicious.
- If the *SSE* test statistics is larger than the threshold, the assumed number of erroneous DOA measurements is increased by 1, i.e. $N_{err} = N_{err} + 1$.

4. Check of N_{err}:
- If $N_{err} \leq N_{err,MAX}$, the process returns to the step 2. $N_{err,MAX}$ is the maximum number of simultaneously erroneous DOA measurements to be considered.
- If $N_{DOA} - N_{err} < 4$, the estimations of the Euler angles obtained with (14) and (15) are not sufficiently accurate for solving (13). The process has to be terminated. The determination of the antenna attitude and detection of potential spoofing/meaconing are declared to be failed.
- If $N_{err} > N_{err,MAX}$, the process is terminated with the same outcome as above.

First initial performance analysis of proposed approach as well as the verification of its software implementation have been carried out with the help of Monte-Carlo simulations in Matlab. The obtained results will be presented in the next section.

PERFORMANCE ASSESSMENT

The Monte-Carlo software simulations have been carried out using an exemplary GPS satellite constellation that is shown in Figure 6 in form of a skyplot. The directions to the ten satellites in the skyplot are used to form the matrix $\mathbf{D}_{enu}$ in (1) that has in this case the size of $[3 \times 10]$.
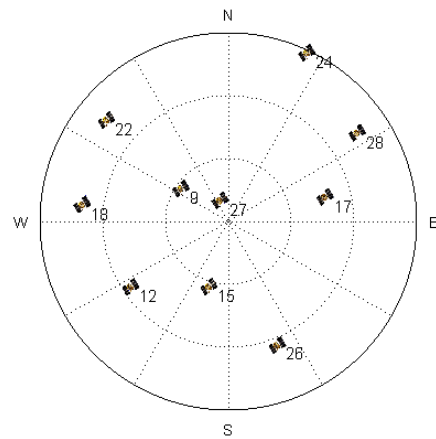

Figure 6: GPS satellite constellation as skyplot in user's ENU coordinate frame

The simulated DOA measurements for all 10000 Monte-Carlo runs are shown in the skyplot in Figure 7. Please note that the actual satellite positions observed by the antenna array (marked with red circles in Figure 7) are different to the satellite positions in Figure 6. This is due to the attitude of the antenna array that was adopted in the simulations as follows: roll angle of 5°, pitch angle of 10°, and yaw angle of 90°. The simulated DOA measurements of a single Monte-Carlo run were used to form the matrix $\mathbf{D}_{loc}$ in (1).

In order to bring the simulated direction of arrival measurements closer to practice, the DOA measurement errors have been simulated with varying standard deviation. The deviation was assumed to depend on the elevation of the satellite in the antenna coordinate frame and followed the curve shown in Figure 8. This approximation is based on the fact that the reception characteristics of planar antenna arrays lead to elevation dependent performance of the DOA estimation. This effect was also observed in the measurement data collected with DLR's GALANT receiver [3], [4] that utilizes a 2-by-2 flat square antenna array and a 2-dimensional unitary ESPRIT algorithm for the direction of arrival estimation [12], [13].
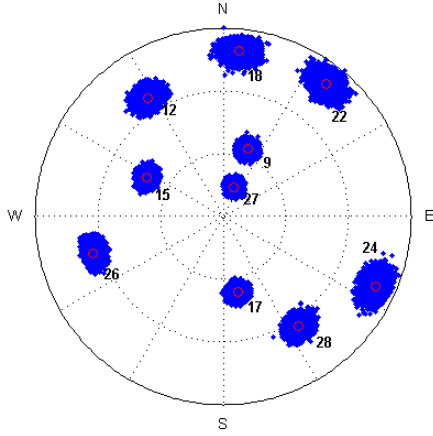
Figure 7: Simulated DOA measurements.
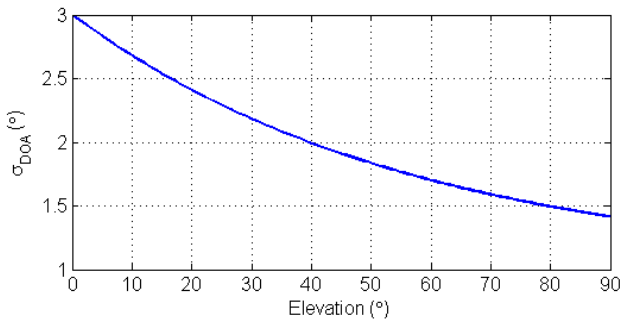Adopted Euler angles are: $r = 5°,\ p = 10°,\ y = 90°$

Figure 8: Approximation of dependency of DOA measurement errors on satellite elevation in antenna coordinate frame

The results for error of estimation of the Euler angles are shown in Figure 9 and Table 1. As it can be observed there, the attitude determination delivers in tested scenario a bias-free estimation of the Euler angles. The standard deviations of the estimation errors have not exceeded 1° for any of the Euler angles.
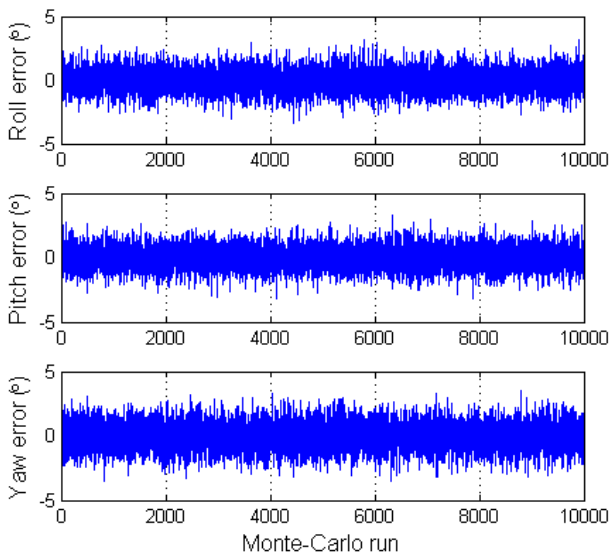
Figure 9: Estimation errors for Euler angles defining the attitude of antenna array

	Yaw	Pitch	Roll
Mean (∘)	-0,022	0.001	0.006
Std. (∘)	0.839	0.804	0.974

Table 1: Mean and standard deviations of attitude estimates obtained for simulated DOA measurements

The probability density function of the obtained SSE test metrics for all 10000 Monte-Carlo runs in shown in Figure 10. As it can be observed in this figure, the pdf estimated from the simulation results matches well the expected theoretical pdf of chi-squared distribution with 17 degrees of freedom (see (18)).
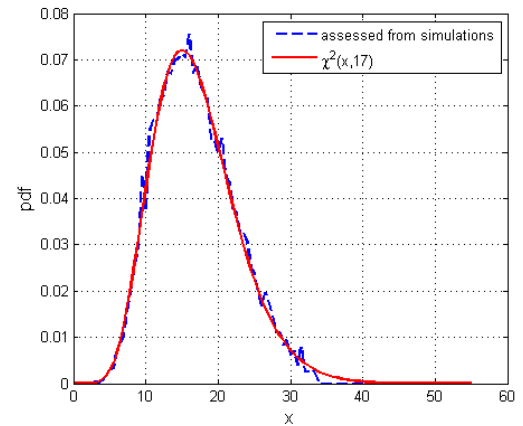

Figure 10: Pdf of SSE test metric

In addition, the Monte-Carlo simulations have been repeated again with the same set-up except of introducing a bias in DOA measurements for the satellite SV17 in order to model the occurrence of false (spoofing) signal. The measurements were biased by -10° for azimuth φ and $-10°$ for elevation θ (see Figure 11).
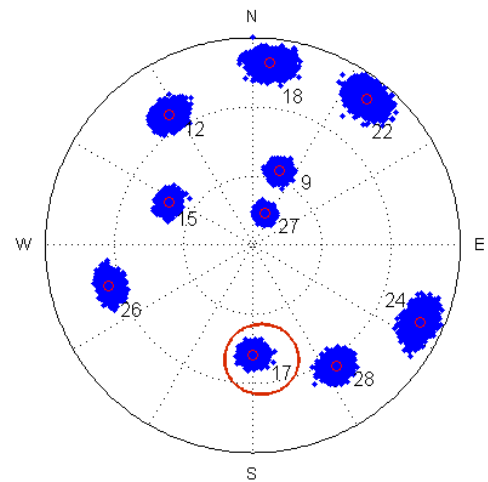

Figure 11: Simulated DOA measurements.
DOA measurements for SV17 are intentionally biased tp model false signal

The introduced bias corresponds to moving away the directional cosines vector $\hat{d}_{loc}$ that defines the estimated direction to SV17 by about 12.5°, i.e. $\Delta_{spoofer} = 12{,}5°$ and $\left(\Delta_{spoofer}/\sigma_n\right)^2 = 34.17$. The corresponding pdfs of the *SSE* test statistics for H_0 and H_1 hypotheses are shown in Figure 12 where good match between the simulation results and predicted theoretical curves can be observed.
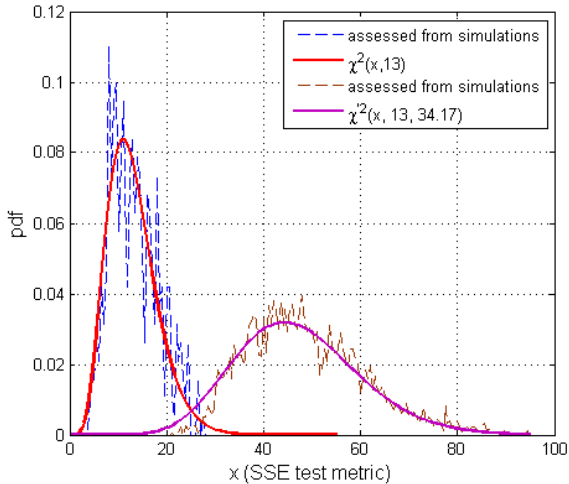

Figure 12: Pdfs of *SSE* test metric for H_0 and H_1 hypotheses

The means and standard deviations of the estimation errors of the Euler angles obtained in the Monte-Carlo simulation with the systematically biased DOA measurement for SV17 are presented in Table 2. Since this wrongful DOA measurement was detected and excluded, the estimation errors of the Euler angles stay un-biased. However, the standard deviations of the estimated Euler angles slightly rise when comparing to the corresponding figures in Table 1. This is due to the fact that the number of DOA measurements used now for the attitude determination has decreased.

	Yaw	Pitch	Roll
Mean (∘)	-0.023	0.077	0.052
Std. (∘)	0.912	0.964	1.071

Table 2: Mean and standard deviations of attitude estimates by using simulated DOA measurements with one biased measurement

In order to validate the assumptions about the underlying statistics of the DOA measurements, the DLR's multi-antenna receiver GALANT [2] is used. Though a simplified version of the attitude determination algorithm described above has been already implemented in real-time in the receiver, the results presented further were obtained in post-processing by using the recorded data. The GALANT receiver supports the NMEA 0183 communication interface that is primarily used to visualize the receiver state parameters in a graphical user interface (GUI). Several proprietary messages have been added to the standard set of NMEA messages in order to support the transmission of the state information regarding the advanced array processing functions of the receiver (adaptive beamforming, direction of arrival estimation) as well as to allow changing of the receiver settings through the GUI. All data required for the attitude determination are already available in the transmitted NMEA messages. A message type GSV contains the DOA information derived for a current user position from the GNSS almanac data. A proprietary NMEA message is used to transmit the estimated DOAs for all GNSS signals in track. The messages of these two types were continuously recorded with the update rate of 1 Hz for GSV message and 10 Hz for the proprietary message over approximately six hours. The antenna array of the GALANT receiver during these tests was mounted statically on the roof of the DLR Institute of Communications and Navigation in Oberpfaffenhofen.

Figure 13 shows the results for estimated roll, pitch and yaw angles whose estimations are based on the recorded real-time measurements as described above. The update rate of the attitude estimation corresponds to the update rate of recorded GSV, i.e. 1 Hz. The mean and standard deviations are shown in Table 3.
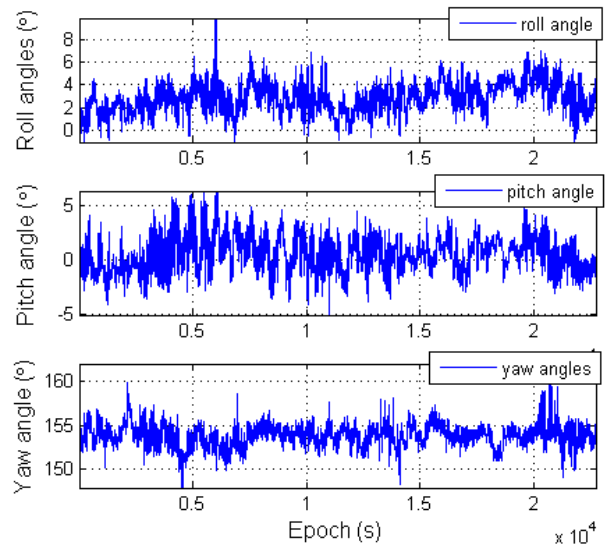

Figure 13: Attitude estimates from post processing of real-time DOA measurements

	Yaw	Pitch	Roll
Mean (∘)	153.840	0.525	2.843
Std. (∘)	1.208	1.608	1.278

Table 3: Mean and standard deviations of the attitude estimates performed on real DOA measurements

In Table 3 it can be observed, that the standard deviations are slightly higher than the assumed parameters of the

Monte-Carlo simulations from above. Furthermore, the results show that the antenna is mounted only with a small inclination, but with a yaw angle of about 153°.

Further results of the post-processing contain the estimated directions of arrival of GNSS signals which were corrected by taking into account the estimated attitude of the antenna array (see Table 3).

As an example, the DOA results for GPS SV 06 are shown in Figure 14. The first two plots show azimuth and elevation angles, where the estimated DOAs and the expected "almanac" DOAs are shown in each plot. As it can be seen in these plots, the estimations of azimuth and elevation angles of arrival are very well centered on the expected values. This indicates that the proposed attitude determination algorithm delivers effectively bias-free results.

The last plot in Figure 14 shows the angle between the vectors of directional cosines corresponding to the estimated and almanac DOAs as defined by (19).As it can be observed in this plot, the variance of the DOA estimation error depends on the elevation of the satellite. Two factors can be responsible for this effect: (i) lower elevation angles result in less signal power and (ii) the planar array geometry limits the resolution available in the direction of arrival estimation.
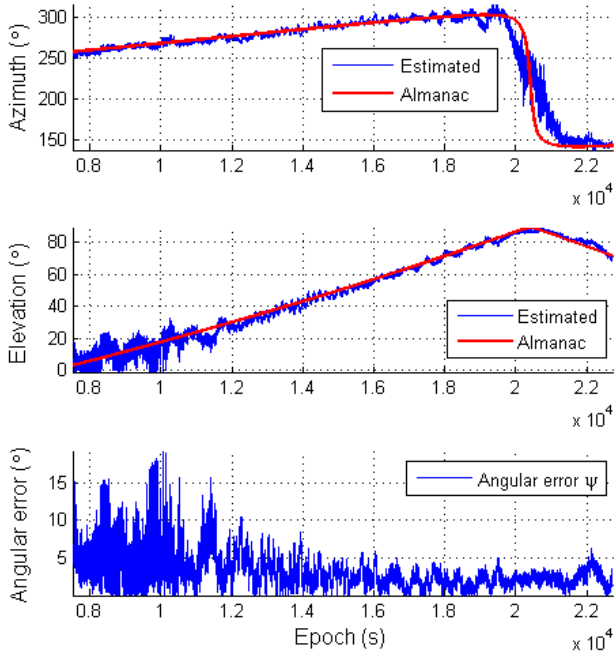

Figure 14: DOA estimation results of SV 06

The results of post-processing indicate an important effect that occurs in a practical system and needs to be carefully taken into account. This effect consists in that for very low elevation angles, the estimated azimuth angles may jump by approximately 180°. A typical behavior of the estimated DOA for a satellite signal experiencing this

effect is shown in Figure 15 for GPS SV 16. The exact reason for this behavior has to be carefully investigated. One of the most probable reasons is the mismatch between the underlying signal model of the ESPRIT algorithm that assumes perfectly identical antenna reception characteristics of all array elements and the actual physical characteristics of the array elements which may be significantly far from being identical due to mutual coupling effect.
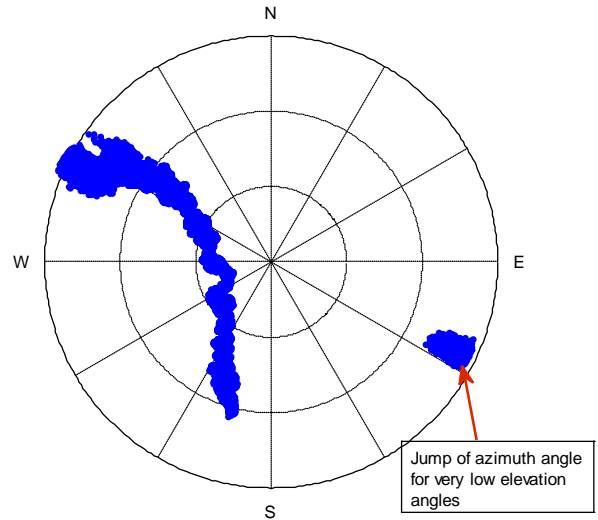

Figure 15: Jumps of azimuth angle in DOA measurements

Because such azimuth angle jumps are treated like a multipath or spoofing effect, the corresponding GNSS signals and their erroneous DOAs are excluded from the process of attitude estimation by the proposed algorithm. The effect of identification of inconsistent DOAs and their exclusion on the number of the DOA measurements used for the attitude estimation process is shown in Figure 16.

SUMMARY AND CONCLUSIONS

In this paper, an approach to joint spoofing detection and antenna array attitude determination has been proposed. It has been shown that the GNSS signals with inconsistent directions of arrival, e.g. spoofing, meaconing or multipath echoes, can be detected and excluded from the attitude determination process. The detection and exclusion are carried out in the way that has many similarities with the multi-hypotheses RAIM techniques. Due to this, the potentially achievable level of performance in term of spoofing/meaconing detection can be easily assessed.

Simulation results demonstrating potentially achievable level of the performance in term of antenna array attitude determination have been presented. The performance of the proposed technique in real environment has been

assessed using DOA-estimation data collected with DLR's proprietary multi-antenna receiver system.

The proposed approach delivers promising results. The performance in real environments has to be analyzed in more detail, which will be the topic of further investigations. In addition, the following research topics can be addressed in the next studies:
(i) improving the DOA estimation more accurate modeling of measurement errors at low elevations;
(ii) considering the use of sequential estimation;
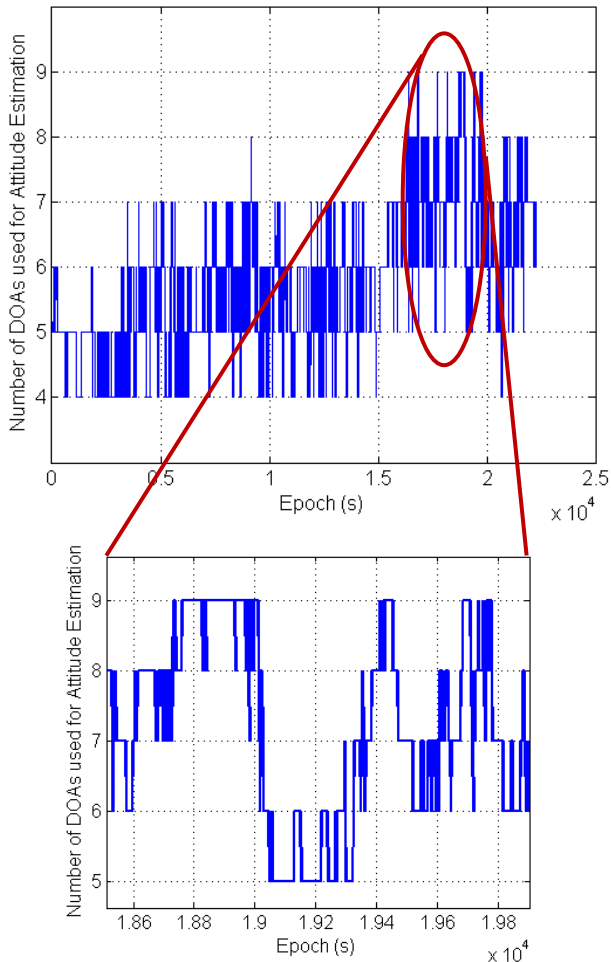(iii) making use of aiding by non-GNSS sensors.

Figure 16: Number of DOA measurements used for attitude determination

REFERENCES
[1]   A. J. Van Dierendonck, "Treatment of re-radiated GNSS," in *Proceedings of Munich Satellite Navigation Summit*, 2009.
[2]   M. V. T. Heckler, M. Cuntz, A. Konovaltsev, L. A. Greda, A. Dreher, and M. Meurer, "Development of Robust Safety-of-Life Navigation Receivers," *IEEE Transactions on Microwave Theory and Techniques*, vol. 59, no. 4, pp. 998–1005, Apr. 2011.
[3]   M. Cuntz, A. Konovaltsev, M. Heckler, A. Hornbostel, L. Kurz, G. Kappen, and T. Noll, "Lessons Learnt: The Development of a Robust Multi-Antenna GNSS Receiver," in *ION GNSS 2010*, 2010.
[4]   M. Cuntz, A. Konovaltsev, M. Sgammini, C. Hättich, G. Kappen, M. Meurer, A. Hornbostel, and A. Dreher, "Field Test: Jamming the DLR Adaptive Antenna Receiver," in *ION GNSS 2011*, 2011, no. 24, pp. 384–392.
[5]   P. Montgomery and T. E. Humphreys, "A Multi-Antenna Defense: Receiver-Autonomous GPS Spoofing Detection," *Inside GNSS*, no. March/April, pp. 40–46, 2009.
[6]   B. S. Pervan, S. P. Pullen, and J. R. Christie, "A Multiple Hypothesis Approach to Satellite Navigation Integrity," *Navigation*, vol. 45, no. 1, pp. 61–84, May 1998.
[7]   B. Hofmann-Wellenhof, H. Lichtenegger, and E. Wasle, *GNSS - Global Navigation Satellite Systems: GPS, GLONASS, Galileo, and more*. Wien: Springer-Verlag, 2007, p. 548.
[8]   F. Markley, "Attitude determination using vector observations and the singular value decomposition," *The Journal of the Astronautical Sciences*, vol. 38, no. 3, pp. 245–258, 1988.
[9]   R. G. Brown, "A Baseline GPS RAIM Scheme and a Note on the Equivalence of Three RAIM Methods," *Navigation*, vol. 39, no. 3, pp. 301–316, Nov. 1992.
[10]   P. B. Ober, "New, Generally Applicable Metrics for RAIM/AAIM Integrity Monitoring," in *Proceedings of the 9th International Technical Meeting of the Satellite Division of The Institute of Navigation (ION GPS 1996)*, 1996, pp. 1677–1686.
[11]   H. L. V. Trees, *Detection, Estimation, and Modulation Theory. Part 1*. Wiley, 2001, p. 720.
[12]   R. Roy, "ESPRIT-estimation of signal parameters via rotational invariance techniques," *IEEE Transactions on Acoustics, Speech and Signal Processing*, vol. 37, no. 7, pp. 984–995, 1989.
[13]   M. Haardt, "Efficient One-, Two-, and Multidimensional High-Resolution Array Signal Processing," Ph.D. dissertation, Technical University of Munich, 1997.